Velocity, Processivity, and Individual Steps of Single Myosin V Molecules in Live Cells

Paolo Pierobon,[†] Sarra Achouri,[†] Sébastien Courty,[‡] Alexander R. Dunn,[§] James A. Spudich,[§] Maxime Dahan,[‡*] and Giovanni Cappello[†*]

[†]Institut Curie, Centre de Recherche, Laboratoire Physico-Chimie Curie, Centre National de la Recherche Scientifique, UMR 168, Université Pierre et Marie Curie-Paris, Paris, France; [‡]Laboratoire Kastler Brossel, Centre National de la Recherche Scientifique, UMR 8552, and Physics and Biology Department, Ecole Normale Supérieure, Université Pierre et Marie Curie-Paris, Paris, France; and [§]Stanford University School of Medicine, Stanford, California

ABSTRACT We report the tracking of single myosin V molecules in their natural environment, the cell. Myosin V molecules, labeled with quantum dots, are introduced into the cytoplasm of living HeLa cells and their motion is recorded at the single molecule level with high spatial and temporal resolution. We perform an intracellular measurement of key parameters of this molecular transporter: velocity, processivity, step size, and dwell time. Our experiments bridge the gap between in vitro single molecule assays and the indirect measurements of the motor features deduced from the tracking of organelles in live cells.

INTRODUCTION

Myosin V is an actin-associated protein, involved in intracellular transport. This molecular motor uses the chemical energy released during adenosine triphosphate (ATP) hydrolysis to produce mechanical work and to carry cargoes through the cytoplasm. The mechano-chemical properties of myosin V have been addressed in great detail by means of several in vitro assays, which allow a fine and independent control of all the parameters (ATP and adenosine diphosphate (ADP) concentration, temperature, force and others) (1), and structural analysis (2–4). Those experiments have shown that myosin V molecules move by taking many consecutive steps in a hand-over-hand manner (5). A combination of single-molecule, optical trapping (6–17), total internal reflection microscopy (5,18,19,20), and bulk kinetics experiments (21–23) have contributed to determine in vitro the mechanistic parameters for myosin V, notably the velocity and length of single processive runs, under a variety of conditions. However, the inherent limit of in vitro assays is that the myosin V is observed out of its natural environment, the cell. The cell is a complex machine, where the pH and the ionic strength are actively regulated and molecular crowding is extreme. In addition, myosin activity might depend on molecular partners, cofactors and other parameters, among which are the local geometry and topology of the cytoskeleton. All these elements might critically affect the motor properties and are often difficult to reproduce in vitro.

So far, experiments aimed at characterizing the intracellular motion of myosin V have been essentially based on the tracking of endosomes, melanosomes, or other organelles inside the cell (24–27). As those objects are transported by molecular motors, the analysis of their motion provides an indirect measurement of the motor activity in its native environment. The main drawback of this approach is that neither the type of motors pulling on a vesicle nor their total amount is unequivocally determined. In fact, the motor family and their number strongly affect the speed, the directionality, and the processivity of the organelle, as well as the maximum force developed during the motion (28).

In this work, our objective is to bridge the gap between the in vitro characterization of myosin V motors and observations of myosin V-driven organelle movement inside the cells. In particular, we aim to determine whether the parameters measured in vitro are consistent with the values measured in vivo and quantify the differences. A clear example of discrepancy between in vitro and in vivo is the speed of the myosin V. While in vitro experiments provide a mean velocity in the range 200–450 nm/s (9,11,22), the tracking of organelles suggests that the myosin V moves at 1 μm/s or faster (24,29). So far, the reason for this discrepancy has remained unclear. It could, for instance, result from a lack of optimization of the in vitro conditions or from insufficient knowledge on the organelles. Another key parameter that can be unequivocally determined only for a single molecule and cannot be deduced from organelles trajectories is the processivity. Measuring the run lengths of single myosin V molecules inside the cell is in fact the only way to access the real in vivo processivity of this motor.

Here we demonstrate an intracellular single-molecule assay, in which individual myosin V motors are introduced into cultured HeLa cells. To track the motion of these myosin V molecules within the cell, we label the motor with a fluorescent reporter. The choice of the reporter is critical: an ideal probe specifically binds to the myosin V without perturbing its activity and is not cytotoxic. In addition, it should be bright and photostable enough to allow fast detection (in the millisecond range) and long observations (up to several minutes). Recent works have shown that semiconductor quantum dots

Submitted November 7, 2008, and accepted for publication February 5, 2009.

*Correspondence: giovanni.cappello@curie.fr or maxime.dahan@lkb.ens.fr

Editor: Claudia Veigel.

0006-3495/09/05/4268/8 $2.00

doi: 10.1016/j.bpj.2009.02.045

(QDs) are good candidates for intracellular experiments (30–33) as they satisfy most of those requirements. In our experiments, we label the myosin V by randomly replacing one of the 12 calmodulins with a biotinylated one (see Fig. 2 *A*) and we use this biotin tag to conjugate the proteins with streptavidin-coated QDs (34) before internalizing the motors into the cytoplasm. Thereby, we directly measure the velocity, processivity, and individual steps of single myosin V molecules moving in the cytoplasm of live cells.

MATERIALS AND METHODS

In vitro motility assay

We use commercial rabbit muscle G-actin (Cytoskeleton) diluted at 2.5 mg/mL. The polymerization is induced by mixing 2 μL of G-actin and 2 μL of ATP (6 mM) in 7.5 μL of Assay Buffer (25 mM imidazole-HCl at pH 7.4, 25 mM KCl, 1 mM EGTA, 10 mM DTT, and 4 mM $MgCl_2$) and incubating 20 min. The F-actin so obtained is stabilized with Alexa Fluor 488 phalloidin (2 μL at 66 μM). The stabilized actin filaments are diluted at 1:100 in assay buffer and introduced in a flow chamber where they bind to the coverslip via myosin II treated with N-ethylmaleimide to inhibit the ATPase site. The chamber is rinsed with Assay Buffer supplemented with 1 mg/mL of bovine serum albumin to prevent nonspecific interaction. Finally the myosin V/Quantum dot constructs (MyoV::QDs) are introduced in the motility buffer (final dilution 10 nM), that, in addition to the assay buffer, contains 2 mM ATP, an oxygen-scavenging system (20 mM D-glucose, 20 μg/mL glucose-oxydase, 8 μg/mL catalase) and ATP regeneration system (40 mM phospho-creatine and 0.1 mg/mL creatine-phosphokinase, following the protocol in (35)). The coverslip is sealed with vaseline, lanoline, and paraffin at 1:1:1. Observations are performed at room temperature (23°C).

Myosin and calmodulin preparation

The chicken myosin V/GCN4 fusion plus calmodulin is expressed and purified as previously described (19,36), with minor modifications. The human essential light chain LC1sa is cloned into the pFastBac vector and converted into a separate virus. Coinfection with the myosin V/calmodulin virus and the LC1sa virus leads to the expression of myosin V bearing both calmodulin and the essential light chain.

A single cysteine is incorporated into sea urchin vertebrate-like calmodulin via the mutation Q143C, and the protein is expressed and purified as previously described (19). Q143C calmodulin is transferred into buffer containing 20 mM imidazole and 5 mM CaCl2, pH 7.5 using a Micro Bio-Spin 6 buffer exchange column (BioRad, Hercules, CA), and diluted to a final protein concentration of 6.7 mg/mL. Biotin-maleimide (Sigma, St. Louis, MO) is prepared as a 50-mM stock solution in dimethylsulfoxide, and added to a final concentration of 0.5 mM. The reaction is then incubated at room temperature for 1 h, then dialyzed against 10 mM imidazole, 0.5 mM EGTA, and 0.5 mM DTT, pH 7.5 overnight at 4°C. Biotinylation is confirmed by MALDI-mass spectroscopy. Aliquots are flash-frozen and stored at −80°C.

Construction of the myosin V/calmodulin

See Dunn and Spudich (34). Biotinylated calmodulin is attached to the MyoV following an established protocol, which yields at most one labeled calmodulin per dimer. One microliter of biotinylated calmodulin is diluted in 3 μL of

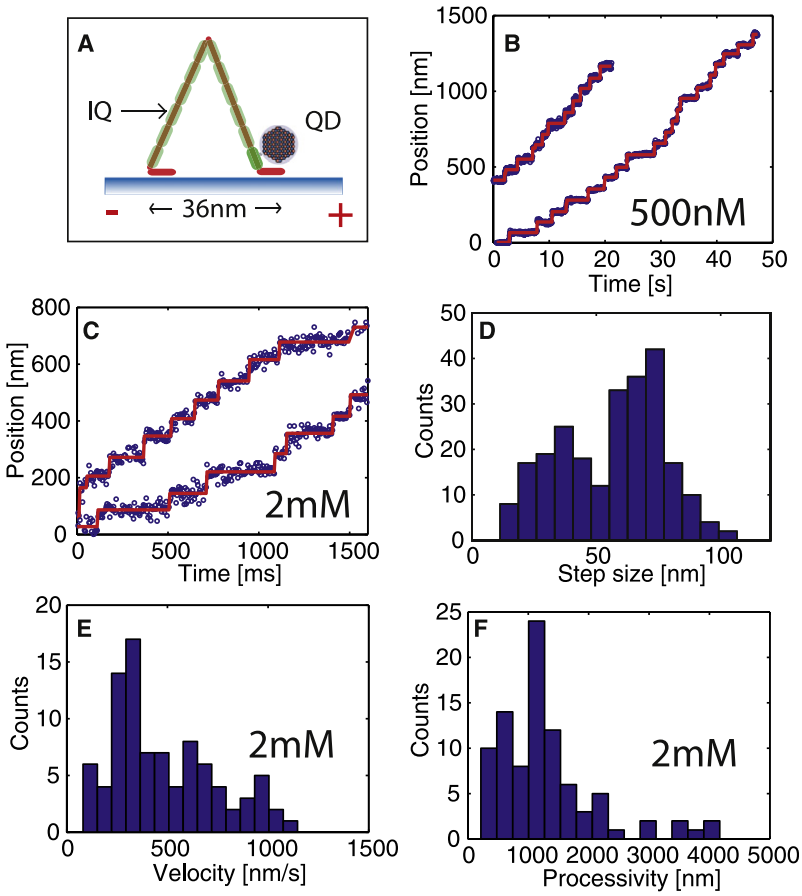

FIGURE 1 (*A*) Cartoon of the myosin V on an actin filament. A quantum dot (QD) is attached to one of the IQ domains of the myosin leg. (*B–F*) Results of the in vitro experiments: (*B*) typical steplike trajectory of a single motor running on an actin filament at [ATP] = 500 nM; (*C*) steplike curves at [ATP] = 2 mM; step-size distribution (*D*), velocity (*E*) and processivity (*F*) of myosin V in vitro at [ATP] = 2mM and low illumination power.

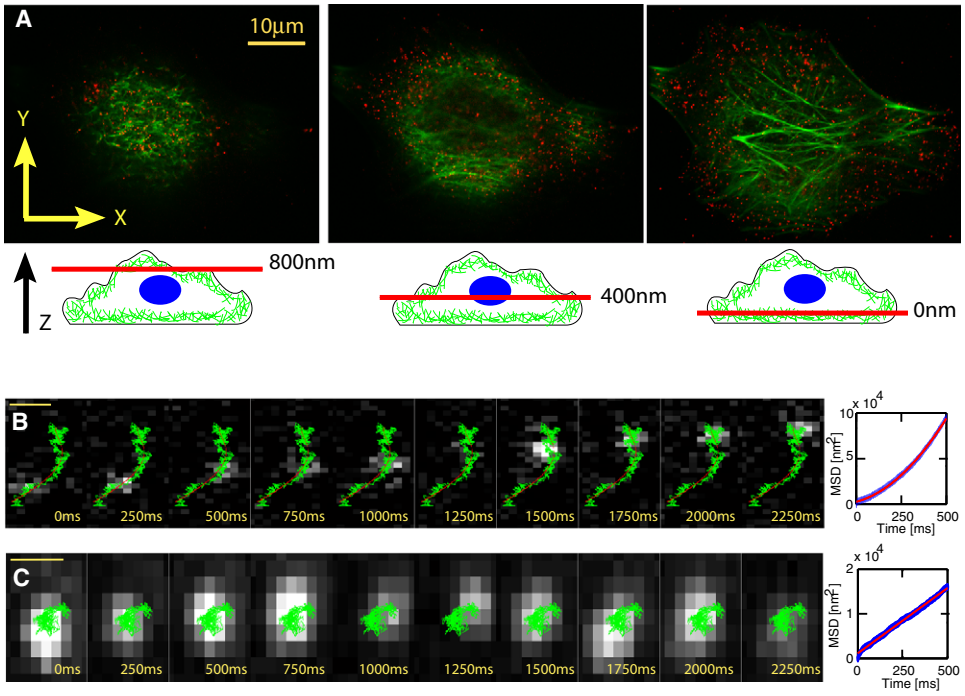

FIGURE 2 (*A*) Three optical sections of a HeLa cell after MyoV::QD internalization. The actin filaments are marked with phalloidin Alexa Fluor 488, while the myosin V is marked with the QDs emitting at 605 nm. The cells are fixed 90 min after the end of the pinocytosis and observed with a spinning disk confocal microscope equipped with a 60× NA 1.4 oil immersion objective. The Alexa Fluor 488 is excited with 491-nm laser and the QDs with a 561-nm laser. The picture shows that most of the QDs are inside the cytoplasm and do not form aggregates. (*B* and *C*) Trajectories of a quantum dot moving in a HeLa cell. The sequence of frames is extracted from a movie acquired at 200 frames per s. The scale is 500 nm in both sequences. The quantum dot in the panel *B* sequence is attached to a myosin V and moves along an actin filaments while the one in panel *C* randomly diffuses through the cytoplasm; QD positions are extracted fitting the point-spread function to a two-dimensional Gaussian with a spatial precision of 10-nm (trajectories in *green*). Directed motions are often curvilinear due to the flexibility of the actin filaments and are therefore fit to a polynomial curve (*right line* on the *top*). (*Right*) Mean-square displacement measurements allow us to discriminate between the one dimension diffusion and progressive motion. (*Red line*) Quadratic (linear) fit of the MSD of the direct (diffusive) trajectory.

Exchange Buffer (EB, 25 mM KCl, 25 mM imidazole, and 4 mM MgCl2, pH 7.5). One microliter of this dilution and 1 μL of MyoV are added to 18 μL of EB and incubated at room temperature for 2 min. Addition of 1 mM of $CaCl_2$ initiates the calmodulin exchange, which is quenched by addition of 8 mM of EGTA after 5 min at room temperature. QD-streptavidin conjugates are purchased from Invitrogen (Carlsbad, CA). The particles are diluted from 2 μM to 100 nM in their buffer (borate buffer) and sonicated twice for 15 s. Four microliters to 16 μL of this dilution and 4 μL of tagged MyoV are added to EB to obtain 40 μL of conjugated MyoV::QD. Steps are observed only when the ratio QD/MyoV is >4.

Intracellular loading of MyoV::QD

See Courty et al. (30) and Okada and Rechsteiner (37). Cell cultures on 30-mm glass coverslips are immersed in the hypertonic medium (94% D-MEM, 5% serum, 1% HEPES, glucose at saturating concentration) with the MyoV::QD construction at concentration 10 nM (40 μL in 360 μL of hypertonic medium) for 12 min, then immersed in the hypotonic medium (60% D-MEM-serum, 40% water MQ) for 2 min and kept in the recovery medium (90% Opti-MEM, 10% serum) for the rest of the observation time.

Data collection and analysis

QD-tagged myosins are imaged using a wide-field epi-fluorescence microscope (Axiovert 100, oil objective 100×, NA 1.40 plus a 2.5× magnifying lens; Carl Zeiss, Oberkochen, Germany) and an amplified CCD camera iXon EM DU860-BV (CCD size 128 × 128 pixels, pixel size 24 μm; Andor Technology, South Windsor, CT). The QDs (emitting at 605 nm) are excited at 532 nm with a laser spot of 15 μm in diameter and intensity 1–4 kW/cm^2. The processivity and the velocity in vitro are measured at lower illumination intensity (~300 W/cm^2) to reduce the blinking of the QDs.

Individual trajectories are extracted from image sequences by means of a homemade particle-tracking program implemented in MatLab (The MathWorks, Natick, MA). After the operator has introduced manually the initial point, the position of a MyoV::QD is determined in each frame by fitting the fluorescent spot with a two-dimensional Gaussian (5,38). The results of the fit are taken as initial conditions for the fit in the following image. In the case of blinking, the program tries to retrace the nanoparticle in the 10 subsequent frames. If the blinking duration exceeds 10 frames, the fitting is stopped and the results analyzed. We use a time resolution of 5 ms, which gives, in vitro, a pointing accuracy of ~10 nm. This localization accuracy, estimated using immobilized QDs, is mainly limited by the total amount of photons supplied by the QD. Stronger illumination and/or longer exposure time would, in principle, improve the tracking precision. However, long exposure times partially hide the myosin stepping while stronger illumination enhances the QD blinking and makes the tracking more difficult.

As the trajectories are often curved, we introduce a curvilinear abscissa to describe the motion of the MyoV::QD. To estimate the analytical expression of the whole trajectory, we fit the position of the center at each time step $(x(t), y(t))$ with two independent polynomials (function of time) of n^{th} degree: $x(t) = a_0 + a_1 t + a_2 t^2 + \ldots + a_n t^n$ and $y(t) = b_0 + b_1 t + b_2 t^2 + \ldots + b_n t^n$. The degree of the polynomials is usually fixed to three but in some cases has to be increased, in particular when the trajectories are very long (see Supporting Material). The trajectories are then projected along the curvilinear abscissa.

Fixation of the cells

Cells are fixed 90 min after QD internalization with a pynocitic influx. The cells are then rinsed with phosphate-buffered saline (PBS) and fixed with 4% paraformaldehyde diluted at 4% for 10 min. The cells are rinsed three times every 5 min with PBS. We subsequently stain the actin filaments incubating the cells 30 min in PBS with bovine serum albumin at 0.1% and fluorescent phalloidin Alexa Fluor 488 at 0.5 μM. Finally, we rinse the cells with PBS every 5 min and mount them on a glass coverslip using Vectashield (Vector Laboratories, Burlingame, CA).

RESULTS

We first verify the activity of the MyoV::QD constructs and check the accuracy and reproducibility of our assays. We perform in vitro experiments in the bead-assay geometry, with a QD instead of a bead (see Materials and Methods) (18). To determine the experimental conditions to observe a single-molecule run, we progressively reduce the MyoV/QD ratio, until the myosin stepping becomes visible, as shown in Fig. 1, *B* and *C*. We define as single-molecule measurement the experiments carried out with this MyoV/QD relative concentration. The experiments are performed with ATP concentrations of 500 nM and 2 mM. At 500 nM ATP, the stepping rate is mainly limited by the ATP on-rate, and the average dwell time, i.e., the mean interval between consecutive steps, is ~4 s (22). At 2 mM ATP, a value close to the physiological concentration, the stepping rate is limited by the ADP release and the dwell time drops to ~160 ms (23). In both ATP conditions, individual steps of the motor are clearly identified (Fig. 1, *B* and *C*).

The step sizes and durations are extracted from the trajectories by means of a step-finding algorithm (*red line* in Fig. 1, *B* and *C*) (39). In many trajectories, we measure an average step size of ~74 nm, which corresponds to the typical distance covered by the myosin V head, labeled with a QD, during the step. We also observe sequences of alternate 30 nm and 40 nm steps (see Fig. 1 *D*). As already mentioned in the literature, such shorter steps result from QDs attached higher up on the lever arm, close to the myosin stalk. We did not observe alternate 20-nm and 50-nm steps, as reported elsewhere (5,34). Since we are interested in comparing the results of in vitro assays with observations in living cells, we determine the velocity and processivity of the myosin V at 2 mM ATP (Fig. 1, *E* and *F*). We find an average run length (± standard error of the mean) of 1.3 ± 0.2 μm ($n = 90$) and an average velocity of 500 ± 30 nm/s ($n = 90$). All these results are in agreement with the literature (5,11,40) and in particular with the measurements made on the same motor tagged with a gold nanoparticle (diameter ~40 nm) (34).

Having demonstrated that the motor protein remains active after QD conjugation and behaves as a single molecule, we focus on experiments in living cells. To ensure a significant comparison between in vitro assays and observations in living cells, both kinds of experiments are carried out in parallel, using the same batch of MyoV::QD and at the same temperature (23°C). The internalization within cells is achieved through osmotic release of pinocytic vesicles (see Materials and Methods), which leads to the uptake of the MyoV::QD by the cells in ~15 min (30). After the pinocytic influx, we let the cells recover for 1 h in the incubator at 37°C. The dynamics of MyoV::QD constructs in the cells is then recorded at room temperature by fluorescence video-microscopy. In the best cases, we observe motility for up to 5 h after pinocytosis. Fig. 2 *A* shows three optical sections of a HeLa cell after MyoV::QD internalization, fixation, and staining of the actin filaments with fluorescent phalloidin (*green filaments*). The images are extracted from a stack acquired with a spinning disk microscope. We observe that most of the MyoV::QDs (*red dots*) are localized in the cytoplasm and very few remain trapped at the cell membrane. No MyoV::QD are observed inside the nucleus. Eventually, we recognize single QDs from aggregates (which are rather rare, as can be seen from Fig. 2 *A*) by their characteristic blinking.

In living cells, we observe two different types of motion. A large fraction of the MyoV::QD freely diffuse in the cytoplasm, while ~5% of them exhibit a direct motion. We interpret the latter events as MyoV::QD running on actin filaments and the former as due to unbound MyoV::QD or unconjugated QDs. In Fig. 2, *B* and *C*, we show two sequences of images, which illustrate the typical movements. The MyoV::QD in Fig. 2 *B* exhibits a directed movement, possibly along an actin filament. As many trajectories occur on actin filaments bent at the micrometer scale, we project the x,y coordinates of the MyoV::QD position on a curvilinear abscissa (*red curve* in Fig. 2 *B*), as detailed in the Materials and Methods. In contrast, the MyoV::QD in the sequence of Fig. 2 *C* seems to randomly diffuse in the cytoplasm. To further analyze the motion, the mean-square displacement (MSD) is computed for both trajectories (*last column* of Fig. 2, *B* and *C*). The MSD for the MyoV::QD above varies quadratically, indicative of a directional movement with an average speed $v = 390 \pm 10$ nm/s. The MSD for the MyoV::QD below is linear, corresponding to a Brownian diffusion with a coefficient $D = 9.8 \pm 0.1 \times 10^{-3}$ μm^2/s. The average diffusion constant measured in the cells with our construct is $D = 1.8 \pm 0.7 \times 10^{-2}$ μm^2/s) ($n = 10$).

We verify that the directed motions are due to the activity of myosin V. To do so, we perform three control experiments in which we internalized:

1. Nonconjugated QDs.
2. QDs coupled with biotinylated calmodulin only.
3. QDs coupled with denaturated myosin V (kept for 2 h at 23°C).

In none of those control experiments do we observe directed motions. This rules out the possibility that the MyoV::QD are trapped in pinosomes, endosomes, or other organelles transiently carried by endogenous motors (e.g., myosin, kinesin, or dynein). Therefore, we consider that the myosin V is responsible for the MyoV::QD motion. In light of recent experiments by Ali et al. (41), showing that myosin V can diffuse on microtubules, we investigate the role of the microtubules on MyoV::QD movement. Upon incubation of the cells with microtubule-depolymerizing drug nocodazole (10 μM), we still observe directed movement of the MyoV::QD, with an average velocity of 630 ± 100 nm/s, close to the one measured in the untreated cells. This rules out the hypothesis that the motion inside the cell originates from a coupling with the microtubules network. To further verify that the motion, we observe results from

myosin V molecules moving along F-actin, as we incubate the cells with 1 μM Latrunculin A for 30 min. No directed motion is observed in these treated cells. Motility is recovered ~1 h after washing Latrunculin A from the medium.

In the following, we focus on the MyoV::QD exhibiting a directed motion. In approximately one-third of the trajectories, we distinguish steps in the motion of the MyoV::QD, as shown in the Fig. 3 *A*. We notice that intracellular tracks exhibit more fluctuations compared to in vitro traces. Several factors possibly account for this additional noise. In cells, the signal/noise ratio in the detection of a single QD is reduced due to the autofluorescence background, leading to a degraded pointing accuracy. In addition, actin filament fluctuations, as well as cell intrinsic motion, might contribute to the noise in the MyoV::QD position and spread the experimental measurements.

The step-size distribution is represented by the histogram in Fig. 3 *B*, from which we compute an average step size of 74 ± 2 nm ($n = 412$). The associated dwell-time distribution is shown in the Fig. 3 *C*. The mean dwell time, computed on 412 events, is 80 ± 5 ms. From our data, we also extract the velocity and the processivity. Fig. 3 *D* shows the speed distribution for 92 tracks, which gives an average value of 710 ± 50 nm/s ($n = 92$). The processivity distribution is shown in Fig. 3 *E* and is characterized by an average value of 2.2 ± 0.2 μm ($n = 92$).

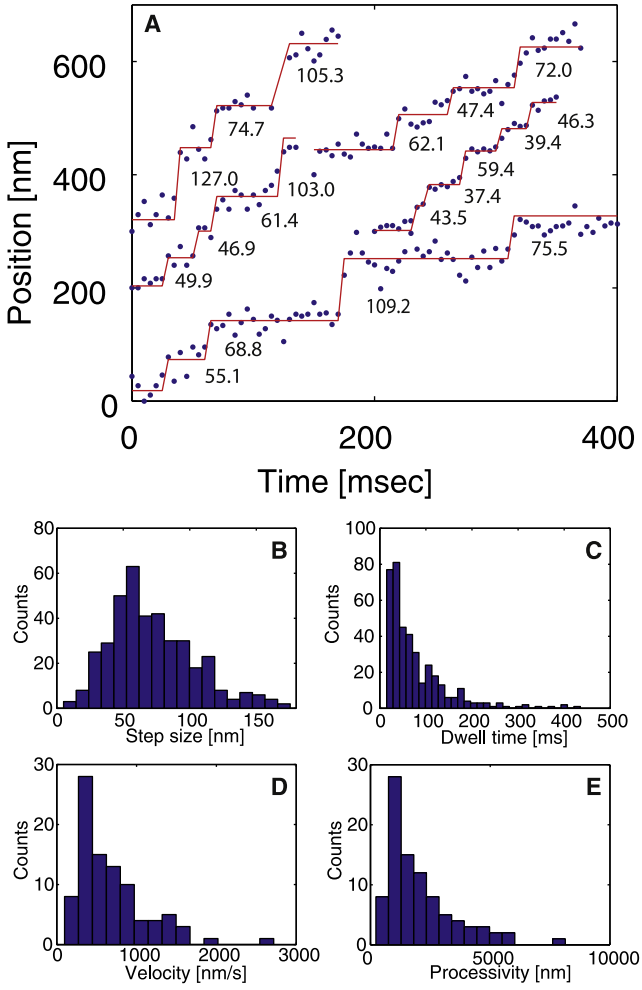

FIGURE 3 Results of the experiments in living cells. (*A*) Examples of the steplike curves observed in the cells (in *red* is the fit performed with the step-finding algorithm). (*B*) Step-size and (*C*) dwell-time distributions. (*D*) Velocity and (*E*) processivity of the motors.

DISCUSSION

General remarks

In our experiments, we develop an assay to investigate the properties of individual myosin V motors in live cells. First, purified myosin V molecules are labeled in vitro. We next verify their functionality after conjugation with a QD. Finally we prove that the motor activity is maintained once introduced in the cytoplasm. In this work, we measure the step size, the dwell-time, the processivity, and the velocity of the myosin V in the cell. Before commenting on the distributions of these different observables, we make some general remarks on our assay.

One could argue that QDs, which have a hydrodynamic diameter at ~30 nm (42), are a probe sufficiently large to significantly affect the motion of the myosin V. We compare the maximal force developed by the myosin V to the viscous drag of a QD carried through the cytoplasm. The viscous force acting on the QD is $F = \frac{k_B T}{D} v$, where D is the diffusion constant, k_B the Boltzmann constant, T the temperature, and v the speed imposed by the myosin V. Given a diffusion coefficient of $D = 1.8 \pm 0.7 \times 10^{-2}$ μm^2/s and a velocity $v = 710$ nm/s, the viscous force is ~0.16 pN. This force is 10-times smaller than the stall force of the myosin V (~2 pN) (11), and therefore, should not perturb the myosin motion.

A second remark concerns the three-dimensional motion of the myosin V. In principle, a correction should be applied to the trajectories that are not parallel to the focal plane. However, when a QD moves out of focus, the width of its fluorescence spot increases. Here we discard trajectories where this broadening is observed. For the trajectories that remain within the depth of field, a simple estimate shows that the effect of three-dimensional movement on the velocity or step-size measurements is minimal. Indeed, if we consider a depth of field of ~500 nm and an average run length of 2 μm, the maximum tilt θ_m of the trajectory is ~15°. Assuming an homogeneous distribution of tilt between $-\theta_m$ and $+\theta_m$, this implies that the processivity, velocity, and step-size are underestimated by no more than 2%, well below our experimental uncertainty. Moreover, the HeLa cells are rather flat (aspect ratio 20:1) and it is much more likely to observe a nearly flat trajectory than a tilted one.

Step size and dwell time

As explained above, the step size and dwell time are extracted from the steplike curves similar to the ones showed

in Figs. 1 and 3. For the analysis, we focus only on the curves where the steps can be visually identified. As a result, we end up with 28 curves (for a total of 412 steps) out of the 92 tracks measured in the cells. We also consider as fake the steps smaller than 10 nm and shorter than 10 ms, because they fall below our experimental resolution. The step-size distribution is shown in Fig. 3 *B*. The mean value of the step size, computed from 412 single steps, is 74 ± 2 nm.

This value coincides exactly with the one expected for a myosin V labeled with QD attached near the head. Actually, this finding is a little surprising given that the distribution results from the superposition of different subpopulations of steps. In addition to motors moving with 74-nm steps, there are also those with alternate 30- and 40-nm steps (or 20- and 50-nm) (5). In contrast to in vitro experiments, our spatial resolution in cells does not permit us to unambiguously distinguish the different kinds of tracks. This partly accounts for the broadening of the distribution.

Another effect also contributes to the width of the distribution and, in particular, to the observation of large steps (>74 nm). As further discussed below, the velocity of the motor in the cell is ~700 nm/s, faster than in vitro. For a 36-nm step, this corresponds to a dwell time of 50 ms. In our measurements (Fig. 3 *C*), we found a mean dwell time of $T = 40 \pm 5$ ms ($n = 412$), in reasonable agreement with the expected value. As a result, there is an increased probability of missing single steps. Indeed, when two or more steps occur within 15 ms (three frames), they appear as a single, larger one. The percentage of steps experimentally missed can be evaluated using Poisson statistics.

The probabilities $P_{n=2}$ and $P_{n=3}$ of having two and three consecutive 36-nm steps within an interval of duration τ, conditionally on the fact that one step occurred, are equal to $a/2$ and $a^2/6$, respectively (with $a = \tau/T$). For $\tau = 15$ ms and $T = 40$ ms, $P_{n=2} \approx 18\%$ and $P_{n=3} \approx 2\%$, meaning that the probability of measuring multiple steps exceeds 20%. A more detailed investigation of myosin V stepping needs higher spatial and temporal resolution. This might require other imaging techniques, probably based on light scattering (43) rather than on fluorescence.

Processivity and velocity

In vitro we find a mean spatial processivity of 1.3 ± 0.2 μm, while it is slightly longer in the cells where the mean value is 2.2 ± 0.2 μm. Both are compatible with the ones reported in the literature (see Table 1). The discrepancy between run length in vitro and intracellularly might be due to the QD blinking that artificially shortens the apparent run length in vitro. In fact, the experiments in vitro that we perform at higher illumination power systematically show shorter processivity. The effect is much weaker inside the cells, where the blinking is noticeably lower, possibly due to the reducing environment in the cytoplasm (32). Alternatively, we might argue that this processivity difference is due to the effect of local viscosity. We can define as the escape time the time t_{esc} needed to diffuse away from the filament over a distance comparable with the myosin length (i.e., 36 nm). In pure water, t_{esc} is ~30 μs for a 30 nm QD. This value is much shorter than the typical binding time of the myosin V head (0.5–2.0 ms (8,34)). As a consequence, when the myosin V releases from the actin filament, the chance of escaping is much higher than rebinding. On the contrary, in the cytoplasm the diffusion coefficient of the QD is reduced by a factor of ~1000, which implies a t_{esc} in the tens of milliseconds range. In that case, when the myosin V unbinds from the actin filament its diffusion is basically limited by the QD diffusion. Thus, the myosin V has a chance to rebind to the actin filament and to increase its apparent processivity. Both in vitro and in the cells, we notice a correlation between the MyoV/QD ratio and the processivity: as expected, QDs with more than one myosin V run over longer distances before unbinding (see Movie S1, Movie S2, and Movie S3, in Supporting Material).

TABLE 1 Comparison of the velocities and processivities found in the literature and measured in this work

	In vitro	Cell (vesicle)	Cell (this work)	Cell (+nocodazole)
Velocity (nm/s)	500 ± 30	n.a.	710 ± 50	630 ± 100
Velocity literature (nm/s)	200 ~450*	450 ~1800†	n.a.	n.a.
Processivity (μm)	1.3 ± 0.2	n.m.	2.2 ± 0.2	2.3 ± 0.2
Processivity literature (μm)	1.0 ~2.4‡	n.m.	n.a.	n.a.

Note that "n.a." means that data are not available; "n.m." indicates data that are not measurable or that do not represent a meaningful observable.
*See Rief et al. (11) and Mehta et al. (11).
†See Levi et al. (29).
‡See Yildiz et al. (5) and Vale and Milligan (40).

Our in vitro velocity is among the highest measured in the literature (i.e., ≃400 nm/s on reconstituted actin filaments suspended between two beads (10), see Table 1). In the cells, the myosin V velocity is slightly higher than in vitro (see Fig. 4 for a comparison, through the cumulative distributions, between in vitro and intracellular velocities). This observation seems counterintuitive, because the cellular crowding and the other proteins bound to the actin filaments are likely to impede the myosin motion, rather than speeding it up (44). As a cause for the discrepancy between the velocities in vitro and in vivo, we can rule out effects like the treadmilling of actin filaments or drift due to global contraction of the cell because both are too slow (~10 nm/s). We cannot exclude an apparent velocity increase caused by sliding between filaments generated by the action of cellular myosin II. However, we suspect that this small discrepancy may be due simply to a lack of optimization of the in vitro single molecule assays. In fact, it is hard to faithfully reproduce the exact conditions (pH, salts, ATP, ADP, and P_i concentrations) in which the proteins operate inside the cell. This supports the need for intracellular single-molecule

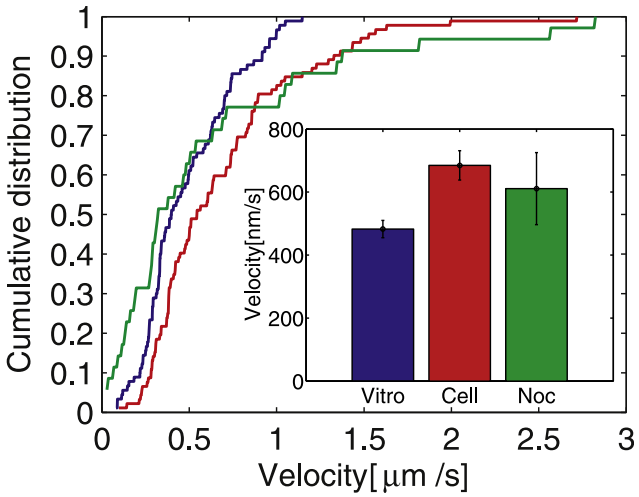

FIGURE 4 Comparison of the velocity cumulative distributions in different experimental conditions. (*Green* and *red lines*) Velocities measured in the cell with and without nocodazole, respectively. (*Blue line*) Speed of cumulative distribution in vitro. (*Inset*) Comparison of the three averages (same color code); error bars represent the standard deviation of the distribution.

experiments, since they provide a more physiologically relevant measurement of the myosin V activity.

Finally, we compare our results with the ones obtained in the cell for another molecular motor: kinesin I. We previously reported (30) that, unlike the myosin V, the kinesin I runs at the same speed in vitro and inside the cell. We also observed that a single kinesin is able to cover, inside the cell, a total distance of several microns, much larger than the distance allowed by its processivity (~1 μm). A careful analysis of the trajectories showed that these long tracks were constituted by a sequence of directed movements, not exceeding the normal processivity of the kinesin, followed by short phases of Brownian diffusion. None of our experiments on the myosin V shows that this molecular motor rebinds to actin filaments shortly after release. The difference observed in the experiments in the cells between those two processive motors may be related to their binding affinity to the filaments on which they run, as well as to the organization of those filaments in the cytoplasm.

CONCLUSION

We report a simple assay to observe the activity of single myosin V in the cytoplasm of living cells. After conjugation to a QD and internalization in the cytoplasm of live HeLa cells, we record the myosin motion with a frame rate of 200 s^{-1} and high spatial resolution. Thereby, we measure the mechanistic parameters of the myosin V in its natural environment, including its velocity, processivity, step size, and dwell time. Compared to in vitro measurements we find slightly increased velocity and processivity. Our observations combine the benefits of a single molecule approach with the complexity intrinsic to living cells and extend the description of the myosin V obtained with in vitro assays. Our approach goes beyond conventional experiments on organelles and opens interesting perspectives for studying intracellular transport pathways and how motors behave in complex filament networks. To further expand the range of applications on intracellular single-molecule experiments, the natural following step will be to directly tag endogenous myosin motors, possibly with an in situ conjugation.

SUPPORTING MATERIAL

Two figures and three movies are available at http://www.biophysj.org/biophysj/supplemental/S0006-3495(09)00603-1.

The authors are grateful to B. Mathieu from the imaging facility at the Ecole Normale Supérieure for his help with the spinning disk microscope, S. De Beco for the fixation protocol, J. M. Kerssemakers for providing the last version of the step-finding algorithm, and A. Roux and D. M. Warshaw for helpful discussions.

G.C. acknowledges the support of STREP "BIOMACH" (grant Nos. NMP4-CT-2003-505-487 and ANR-05-NANO-045). M.D. is supported by grant No. ANR-05-NANO-045 and Fondation pour la Recherche Médicale. J.A.S. is supported by grant No. GM33289 from the National Institutes of Health. A.R.D. was supported by an American Heart Association postdoctoral fellowship and holds a Career Award at the Scientific Interface from the Burroughs Wellcome Fund.

REFERENCES

1. Sellers, J. R., and C. Veigel. 2006. Walking with myosin V. *Curr. Opin. Cell Biol.* 18:68–73.
2. Walker, M. L., S. A. Burgess, J. R. Sellers, F. Wang, J. A. Hammer, et al. 2000. Two-headed binding of a processive myosin to f-actin. *Nature.* 405:804–807.
3. Burgess, S., M. Walker, F. Wang, J. R. Sellers, H. D. White, et al. 2002. The prepower stroke conformation of myosin V. *J. Cell Biol.* 159: 983–991.
4. Coureux, P. D., A. L. Wells, J. Ménétrey, C. M. Yengo, C. A. Morris, et al. 2003. A structural state of the myosin V motor without bound nucleotide. *Nature.* 425:419–423.
5. Yildiz, A., J. N. Forkey, S. A. McKinney, T. Ha, Y. E. Goldman, et al. 2003. Myosin V walks hand-over-hand: single fluorophore imaging with 1.5-nm localization. *Science.* 300:2061–2065.
6. Veigel, C., S. Schmitz, F. Wang, and J. R. Sellers. 2005. Load-dependent kinetics of myosin-V can explain its high processivity. *Nat. Cell Biol.* 7:861–869.
7. Gebhardt, J. C., A. E. Clemen, J. Jaud, and M. Rief. 2006. Myosin-V is a mechanical ratchet. *Proc. Natl. Acad. Sci. USA.* 103:8680–8685.
8. Cappello, G., P. Pierobon, C. Symonds, L. Busoni, C. Gebhardt, et al. 2007. Myosin V stepping mechanism. *Proc. Natl. Acad. Sci. USA.* 104:15328–15333.
9. Rief, M., R. S. Rock, A. D. Mehta, M. S. Mooseker, R. E. Cheney, et al. 2000. Myosin-V stepping kinetics: a molecular model for processivity. *Proc. Natl. Acad. Sci. USA.* 97:9482.
10. Ali, M. Y., S. Uemura, K. Adachi, H. Itoh, K. Kinosita, et al. 2002. Myosin V is a left-handed spiral motor on the right-handed actin helix. *Nat. Struct. Biol.* 9:464–467.
11. Mehta, A. D., R. S. Rock, M. Rief, J. A. Spudich, M. S. Mooseker, et al. 1999. Myosin-V is a processive actin-based motor. *Nature.* 400:590–593.
12. Veigel, C., F. Wang, M. L. Bartoo, J. R. Sellers, and J. E. Molloy. 2002. The gated gait of the processive molecular motor myosin V. *Nat. Cell Biol.* 4:59–65.

13. Sakamoto, T., A. Yildez, P. R. Selvin, and J. R. Sellers. 2005. Step-size is determined by neck length in myosin V. *Biochemistry*. 44:16203–16210.

14. Clemen, A. E.-M., M. Vilfan, J. Jaud, J. Zhang, M. Barmann, et al. 2005. Force-dependent stepping kinetics of myosin-V. *Biophys. J*. 88:4402–4410.

15. Purcell, T. J., H. L. Sweeney, and J. A. Spudich. 2005. A force-dependent state controls the coordination of processive myosin V. *Proc. Natl. Acad. Sci. USA*. 102:13873–13878.

16. Uemura, S., H. Higuchi, A. O. Olivares, E. M. De La Cruz, and S. Ishiwata. 2004. Mechanochemical coupling of two substeps in a single myosin V motor. *Nat. Struct. Mol. Biol*. 11:877–883.

17. Moore, J. R., E. B. Krementsova, K. M. Trybus, and D. M. Warshaw. 2001. Myosin V exhibits a high duty cycle and large unitary displacement. *J. Cell Biol*. 155:625–635.

18. Warshaw, D. M., G. G. Kennedy, S. S. Work, E. B. Krementsova, S. Beck, et al. 2005. Differential labeling of myosin V heads with quantum dots allows direct visualization of hand-over-hand processivity. *Biophys. J*. 88:L30–L32.

19. Churchman, L. S., Z. Okten, R. S. Rock, J. F. Dawson, and J. A. Spudich. 2005. Single molecule high-resolution colocalization of Cy3 and Cy5 attached to macromolecules measures intramolecular distances through time. *Proc. Natl. Acad. Sci. USA*. 102:1419–1423.

20. Syed, S., G. E. Snyder, C. Franzini-Armstrong, P. R. Selvin, and Y. E. Goldman. 2006. Adaptability of myosin V studied by simultaneous detection of position and orientation. *EMBO J*. 25:1795–1803.

21. Rosenfeld, S. S., and H. L. Sweeney. 2004. A model of myosin V processivity. *J. Biol. Chem*. 279:40100–40111.

22. De La Cruz, E. M., A. L. Wells, S. S. Rosenfeld, E. M. Ostap, and H. L. Sweeney. 1999. The kinetic mechanism of myosin V. *Proc. Natl. Acad. Sci. USA*. 96:13726–13731.

23. De La Cruz, E. M., H. L. Sweeney, and E. M. Ostap. 2000. ADP inhibition of myosin V ATPase activity. *Biophys. J*. 79:1524–1529.

24. Schott, D. H., R. N. Collins, and A. Bretscher. 2002. Secretory vesicle transport velocity in living cells depends on the myosin-V lever arm length. *J. Cell Biol*. 156:35–39.

25. Xie, X. S., J. Yu, and W. Y. Yang. 2006. Living cells as test tubes. *Science*. 312:228–230.

26. Kural, C., A. S. Serpinskaya, Y.-H. Chou, R. D. Goldman, V. I. Gelfand, et al. 2007. Tracking melanosomes inside a cell to study molecular motors and their interaction. *Proc. Natl. Acad. Sci. USA*. 104:5378–5382.

27. Levi, V., and E. Gratton. 2007. Exploring dynamics in living cells by tracking single particles. *Cell Biochem. Biophys*. 48:1–15.

28. Ross, J. L., H. Shuman, E. L. Holzbaur, and Y. E. Goldman. 2008. Kinesin and dynein-dynactin at intersecting microtubules: motor density affects dynein function. *Biophys. J*. 94:3115–3125.

29. Levi, V., V. I. Gelfand, A. S. Serpinskaya, and E. Gratton. 2006. Melanosomes transported by myosin-V in *Xenopus* melanophores perform slow 35-nm steps. *Biophys. J*. 90:L07–L09.

30. Courty, S., C. Luccardini, Y. Bellaiche, G. Cappello, and M. Dahan. 2006. Single quantum dot tracking of individual kinesins in live cells. *Nano Lett*. 6:1491–1495.

31. Dahan, M., S. Lévi, C. Luccardini, P. Rostaing, B. Riveau, et al. 2003. Diffusion dynamics of glycine receptors revealed by single-quantum dot tracking. *Science*. 302:442–445.

32. Nan, X., P. A. Sims, P. Chen, and X. S. Xie. 2005. Observation of individual microtubule motor steps in living cells with endocytosed quantum dots. *J. Phys. Chem. B*. 109:24220–24224.

33. Michalet, X., F. F. Pinaud, L. A. Bentolila, J. M. Tsay, S. Doose, et al. 2005. Quantum dots for live cells, in vivo imaging, and diagnostics. *Science*. 307:538–544.

34. Dunn, A. R., and J. A. Spudich. 2007. Dynamics of the unbound head during myosin V processive translocation. *Nat. Struct. Mol. Biol*. 14:246–248.

35. Gèrard, A., S. E. Polo, D. Roche, and G. Almouzni. 2006. Methods for studying chromatin assembly coupled to DNA repair. *Methods Enzymol*. 409:358–374.

36. Sweeney, H. L., S. S. Rosenfeld, F. Brown, L. Faust, J. Smith, et al. 1998. Kinetic tuning of myosin via a flexible loop adjacent to the nucleotide binding pocket. *J. Biol. Chem*. 273:6262–6270.

37. Okada, C. Y., and M. Rechsteiner. 1982. Introduction of macromolecules into cultured mammalian cells by osmotic lysis of pinocytic vesicles. *Cell*. 29:33–41.

38. Gelles, J., B. J. Schnapp, and M. P. Sheetz. 1988. Tracking kinesin-driven movements with nanometer-scale precision. *Nature*. 331:450–453.

39. Kerssemakers, J. W. J., E. L. Munteanu, L. Laan, T. L. Noetzel, M. E. Janson, et al. 2006. Assembly dynamics of microtubules at molecular resolution. *Nature*. 442:709–712.

40. Vale, R. D., and R. A. Milligan. 2000. The way things move: looking under the hood of molecular motor proteins. *Science*. 288:88–95.

41. Ali, M. Y., E. B. Krementsova, G. G. Kennedy, R. Mahaffy, T. D. Pollard, et al. 2007. Myosin Va maneuvers through actin intersections and diffuses along microtubules. *Proc. Natl. Acad. Sci. USA*. 104:4332–4336.

42. Luccardini, C., C. Tribet, F. Vial, V. Marchi-Artzner, and M. Dahan. 2006. Size, charge, and interactions with giant lipid vesicles of quantum dots coated with an amphiphilic macromolecule. *Langmuir*. 22:2304–2310.

43. Nan, X., P. A. Sims, and X. S. Xie. 2008. Organelle tracking in a living cell with microsecond time resolution and nanometer spatial precision. *ChemPhysChem*. 9:707–712.

44. Seitz, A., and T. Surrey. 2006. Processive movements of single kinesins on crowded microtubules visualized using quantum dots. *EMBO J*. 25:267–277.